Regulation of Plasticity and Fibrogenic Activity of Trabecular Meshwork Cells by Rho GTPase Signaling

Padmanabhan P Pattabiraman[1], **Rupalatha Maddala**[1], and **Ponugoti Vasantha Rao**[1,2,*]

[1]Department of Ophthalmology, Duke University School of Medicine, Durham, NC 27710

[2]Department of Pharmacology and Cancer Biology, Duke University School of Medicine, Durham, NC. 27710

Abstract

Glaucoma, a prevalent blinding disease is commonly associated with increased intraocular pressure due to impaired aqueous humor (AH) drainage through the trabecular meshwork (TM). Although increased TM tissue contraction and stiffness in association with accumulation of extracellular matrix (ECM) are believed to be partly responsible for increased resistance to AH outflow, the extracellular cues and intracellular mechanisms regulating TM cell contraction and ECM production are not well defined. This study tested the hypothesis that sustained activation of Rho GTPase signaling induced by lysophosphatidic acid (LPA), TGF-β and connective tissue growth factor (CTGF) influences TM cell plasticity and fibrogenic activity which may eventually impact resistance to AH outflow. Various experiments performed using human TM cells revealed that constitutively active RhoA (RhoAV14), TGF-β2, LPA and CTGF significantly increase the levels and expression of Fibroblast Specific Protein-1 (FSP-1), α-smooth muscle actin (αSMA), collagen-1A1 and secretory total collagen, as determined by q-RT-PCR, immunofluorescence, immunoblot, flow cytometry and the Sircol assay. Significantly, these changes appear to be mediated by Serum Response Factor (SRF), myocardin-related transcription factor (MRTF-A), Slug and Twist-1, which are transcriptional regulators known to control cell plasticity, myofibroblast generation/activation and fibrogenic activity. Additionally, the Rho kinase inhibitor-Y27632 and anti-fibrotic agent-pirfenidone were both found to suppress the TGF-β2-induced expression of αSMA, FSP-1 and collagen-1A1. Taken together, these observations demonstrate the significance of RhoA/Rho kinase signaling in regulation of TM cell plasticity, fibrogenic activity and myofibroblast activation, events with potential implications for the pathobiology of elevated intraocular pressure in glaucoma patients.

Keywords

Glaucoma; Trabecular meshwork; Aqueous humor; Intraocular pressure; Fibrosis; Plasticity; Serum response factor; Slug; Rho GTPase

INTRODUCTION

Glaucoma is a prevalent blinding disease with characteristic optic disc and visual field changes. Elevated intraocular pressure (IOP) due to increased resistance to aqueous humor (AH) drainage through the trabecular pathway is a definite risk factor for primary open-

*Correspondence: P Vasantha Rao, Ph.D, Department of Ophthalmology, Duke University School of Medicine, Durham, NC 27710; Phone: 919-681-5883; Fax: 919-684-8983, rao00011@mc.duke.edu.

The authors confirm that there are no conflicts of interest.

angle glaucoma, the most common form of glaucoma in the United States (Kwon et al., 2009; Weinreb and Khaw, 2004). While there is a general agreement that increased resistance to AH outflow through the trabecular pathway consisting of the trabecular meshwork (TM), juxtacanalicular connective tissue (JCT) and Schlemm's canal (SC), is the primary cause for increased IOP in glaucoma patients, little is known about the etiology of increased resistance to AH outflow (Gabelt and Kaufman, 2005; Keller et al., 2009; Tamm and Fuchshofer, 2007). Previous work from our laboratory and others have demonstrated that the Rho/Rho kinase signaling pathway plays a significant role in regulating AH outflow via the trabecular pathway(Honjo et al., 2001; Rao et al., 2001; Rao et al., 2005; Zhang et al., 2008). Additionally, multiple studies have identified a crucial role for various physiological agents including bioactive lipids (LPA and sphingosine-1-phosphate), endothelin-1, autotaxin, CTGF and TGF-β2 in regulating TM cell contractile tension, cell adhesive interactions, extracellular matrix (ECM) synthesis and αSMA expression, and AH outflow via activation of Rho/Rho kinase signaling and other cellular mechanisms (Fuchshofer and Tamm, 2012; Iyer et al., 2012a; Iyer et al., 2012b; Junglas et al., 2012; Mettu et al., 2004; Nakamura et al., 2002; Pattabiraman and Rao, 2010; Rao et al., 2005; Wiederholt et al., 2000; Zhang et al., 2008). However, we have yet to decipher the specific molecular mechanism(s) by which the effects of Rho GTPase activation or Rho kinase inhibition on AH outflow facility are manifested.

Trabecular meshwork tissue from glaucomatous eyes has been reported to exhibit accumulation of sheath-like plaque material and alterations in ECM organization, accumulation and turnover (Keller et al., 2009; Lutjen-Drecoll et al., 1986; Tamm and Fuchshofer, 2007; Tektas and Lutjen-Drecoll, 2009; Yue, 1996). Furthermore, it is widely believed that changes in biomechanical properties of TM tissue such as tissue stiffness and contraction could lead to increased resistance to AH outflow and elevated IOP (McKee et al., 2011; Pattabiraman and Rao, 2010; Russell and Johnson, 2012). Interestingly, TM tissue has been reported to express αSMA and contain myofibroblast-like cells (de Kater et al., 1992; Flugel et al., 1991; Keller et al., 2009; Tamm et al., 1996). The origin and activation of αSMA expressing and matrix producing cells in TM tissue and their role in ECM deposition and contraction, and in AH outflow resistance, however is not clear. Based on the known effects of activated Rho GTPase and Rho kinase inhibitors on the contractile properties of TM cells, αSMA expression, ECM accumulation in the outflow pathway and on AH outflow, (Mettu et al., 2004; Pattabiraman and Rao, 2010; Rao et al., 2001; Rao et al., 2005; Zhang et al., 2008) we reasoned that sustained activation of the Rho GTPase activity by TGF-β, LPA, Endothelin-1 and CTGF (Junglas et al., 2012; Mettu et al., 2004; Nakamura et al., 2002; Rao et al., 2005; Rosenthal et al., 2005) might represent a key early event in inducing transition of a proportion of TM or SC cells into matrix and αSMA producing myofibroblast-like contractile cells. To address this possibility, we asked whether the TM cells undergo a process similar to epithelial-to-mesenchymal transition (EMT) or endothelial-to-mesenchymal transition (EndMT) by aberrant activation of Rho/Rho kinase signaling leading to changes in cell contractile activity, stiffness and ECM production, eventually influencing the resistance to AH outflow. The role of EMT and EndMT in development and progression of fibrosis has been extensively investigated in different tissues (Kalluri and Neilson, 2003; Kalluri and Weinberg, 2009; Zeisberg et al., 2007). Importantly, both TGF-β and Rho GTPase have been reported to have a critical and interdependent role in regulating both EMT and EndMT and expression of transcription factors (e. g. Snail, Slug, MRTF and Twist) which are critical for cell plasticity and fate transition during these processes (Bhowmick et al., 2001; Cho and Yoo, 2007; Kalluri and Weinberg, 2009; Masszi et al., 2003; Mihira et al., 2012; Zeisberg et al., 2007; Zeisberg and Kalluri, 2013). Additionally, Rho GTPase and TGF-β-induced cell tension and ECM rigidity is known to influence cell plasticity and fate transition in various cell types (Arnsdorf et al., 2009; McBeath et al., 2004).

Based on these different observations, this study evaluated the effects of activated RhoA, Rho kinase inhibitors, TGF-β2, LPA and CTGF on the expression profile of myofibroblast and fibrogenic biomarkers in human TM cells, to seek insights into their mechanistic involvement in increased resistance to AH outflow in glaucoma eyes via aberrant TM cell plasticity and fibrogenic activity. This study provides experimental evidence for the propensity of mesenchyme derived endothelial-like TM cells to transdifferentiate into αSMA, FSP-1 and collagen-1 expressing myofibroblast-like cells upon sustained activation of Rho GTPase signaling.

MATERIALS AND METHODS

Materials

The following reagents were obtained from the respective commercial vendors. Oleoyl-L-α-Lysophosphatidic acid sodium salt (LPA), human recombinant transforming growth factor-β2 (TGF-β2), mouse monoclonal antibodies against α-tubulin, α-SMA, β-actin, vimentin, alpha-smooth muscle actin (Cy3 conjugated) and rabbit anti-β–catenin from Sigma-Aldrich (St. Louis, MO); rabbit anti-Fibroblast Specific Protein (FSP-1) antibody from EMD Millipore (Billerica, MA); rabbit anti-collagen-1 antibody from Abcam (Cambridge, MA); rabbit anti-SMAD2/3 and goat anti-β-tubulin from Santa Cruz Biotechnology (Santa Cruz, CA); CCG1423 from Cayman Chemicals (Ann Arbor, MI); Phospho-SMAD3 antibody from Cell Signaling Technology (Danvers, MA); human recombinant CTGF from Cell Sciences (Canton, MA); Cell permeable C3 transferase from Cytoskeleton, Inc (Denver, CO); SIS3 from Calbiochem (Gibbstown, NJ); Y-27632 and Pirfenidone from Tocris Bioscience (Bristol, UK); Hoechst 33258 from Invitrogen (Carlsbad, CA); protease inhibitor cocktail tablets (complete, Mini, EDTA-free) and (PhosSTOP) from Roche (Basel, Switzerland); Alexa fluor 594 goat-anti-rabbit antibody from Invitrogen (Carlsbad, CA) and monoclonal antibody against myc tag 9E10 from Developmental Studies Hybridoma Bank (Iowa City, Iowa). Rabbit anti-GFP and rabbit anti-Fibronectin antibodies were provided by the laboratories of Daniel Stamer and Harold Erickson, from Duke University, respectively.

Cell cultures

Human TM cells (HTM) were cultured from TM tissue isolated from the leftover donor corneal rings after they had been used for corneal transplantation at the Duke Ophthalmology clinical service as described previously by us (Pattabiraman and Rao, 2010). HTM cells were cultured in Dulbecco's Modified Eagle's Medium (DMEM) containing 10% fetal bovine serum (FBS) and penicillin (100U/500ml)-streptomycin (100μg/500ml)-glutamine (4mM). All experiments were conducted using confluent cultures between four and six passages. All cell culture experiments were performed after serum starvation for at least 24 h unless mentioned otherwise.

Adenovirus-mediated Gene Transduction

Replication defective recombinant adenoviral vectors encoding either GFP alone or constitutively active RhoA (RhoAV14) and GFP provided by Patrick Casey, Department of Pharmacology and Cancer Biology, Duke University School of Medicine, or short hairpin RNA against SRF (Ad-shSRF) or the control adenovirus expressing shRNA against GFP (Ad-shGFP) provided by Joseph Miano from University of Rochester School of Medicine, were amplified and purified as we described earlier (Zhang et al., 2008). HTM cells grown either on gelatin-coated glass coverslips or in plastic petri dishes were infected with adenovirus for the various experiments at 50 MOI (multiplicity of infection). When cells showed adequate transfection (>80%, as assessed based on GFP fluorescence) usually after 24-36 h, they were serum starved for 36 h prior to the experiments.

Plasmid transfection

pcDNA3.1 plasmids expressing the constitutively active RhoAV14 (gift from Patrick Casey, Duke University), EGFP-MRTF-A (gift from Christopher Mack, Department of Pathology, UNC, Chapel Hill) or Myc-tagged Slug purchased from Adgene (Cambridge, MA) were amplified and purified using Qiagen Plasmid *Plus* Maxi Kit (Qiagen, San Jose, CA). HTM cells were transfected with respective plasmids or control EGFP-C1 plasmid using an endothelial Nucleofector Kit (Lonza, Basel, Switzerland) as per the manufacturer's instructions. Transfected cells were plated either on gelatin-coated glass coverslips or in plastic petri-plates. GFP based visualization was used to determine the transfection efficiency and cells transfected at > 80% efficiency were used. Cell morphological changes were recorded, after which the cells were fixed and immunostained or lysed for immunoblot analysis for proteins of interest or processed for RNA extraction for subsequent RT-PCR analysis.

RT-PCR and Quantitative RT-PCR (q-PCR)

Total RNA extracted from HTM cells (control and treated) using the RNeasy Mini Kit (Qiagen, Valencia, CA) was quantitated using NanoDrop 2000 UV-Vis Spectrophotometer (Thermo Scientific, Wilmington, DE). Equal amounts of RNA (DNA free) were then reverse transcribed using the Advantage RT-for-PCR kit (Clonetech, Mountain View, CA) according to the manufacturer's instructions. Controls lacking reverse transcriptase (RT) were included in the RT-PCR experiments. PCR amplification was performed on the resultant RT-derived single stranded cDNA using sequence-specific forward and reverse oligonucleotide primers for the indicated genes (Table 1). For semi-quantitative RT-PCR, the amplification was performed using C1000 Touch Thermocycler (Biorad) with a denaturation step at 94°C for 4 minutes, followed by 94°C for 1 minute, 56°C to 60°C for 60 seconds, and 72°C for 30 seconds. The cycle was repeated 25-30 times with a final step at 72°C for 7 minutes. The resulting DNA products were separated on 1% agarose gels and visualized by staining with ethidium bromide using a Fotodyne Trans-illuminator (Fotodyne Inc., Hartland, WI). GAPDH amplification was used to normalize the cDNA content of control and treated samples in all the PCR reactions.

For q-PCR, the above prepared single stranded cDNA libraries were used in the PCR master mix consisting of iQSYBR Green Supermix (Bio-Rad, Hercules, CA) and gene specific oligo nucleotides. PCR reactions were done in triplicate using the following protocol: 95°C for 2 min followed by 50 cycles of 95°C for 15 seconds, 60°C for 15 seconds, and 72°C for 15 seconds. An extension step was used to measure the increase in fluorescence and melting curves obtained immediately after amplification by increasing temperature in 0.4°C increments from 65°C for 85 cycles of 10 seconds each (iCycler software; Bio-Rad). The fold difference in expression of Twist1, Slug, Snail, FSP-1, Col1A1, and αSMA between control and RhoAV14 or MRTF-A expressing cells was calculated by the comparative threshold (Ct) method, as described by the manufacturer (Prism 7700 Sequence Detection System; Applied Biosystem, Inc).

For miRNA expression studies, total RNA was isolated using mirVana miRNA isolation kit as described by the manufacturer (Invitrogen, Carlsbad, CA). The RNA concentration and purity was verified by measuring UV absorbance (at A260 and A280 nm) using NanoDrop 2000 UV-Vis Spectrophotometer. Total RNA (10 ng) was reverse transcribed into cDNA using TaqMan microRNA reverse transcription kit (TaqMan; Ambion, Austin, TX) with specific and validated primers (TaqMan) for mature miRNA-21 (hs-mir21), miRNA-29a (hs-mir29a) and b (hs-mir29b) and RNU26 (Applied Biosystems, Foster City, CA). q-PCR for mature miRNA-21, miRNA-29a and b and internal control RNU26 was performed according to the manufacturer's instructions using TaqMan Universal MasterMix (TaqMan,

Applied Biosystems). Relative fold changes in miRNA expression between control and experimental groups were determined using the $2^{-\Delta\Delta Ct}$ method.

Immunofluorescence staining

The HTM cells were grown on gelatin (2%)-coated glass coverslips until they attained confluency. After appropriate treatments, cells were washed in PBS twice and then fixed, permeabilized and immunostained for αSMA, collagen-1A1 and FSP-1 as we described previously (Pattabiraman and Rao, 2010). The slides were viewed and imaged using a Nikon Eclipse 90i confocal laser-scanning microscope.

Counting of FSP-1 immuno-positive cells

To assess quantitative changes in the number of FSP-1 immunopositive cells, HTM cells were analyzed by immunostaining for FSP-1 positivity. Quantitation included capturing of images for cell counts from four fields in four quadrants of the coverslip with a minimum of 50 cells/field, based on Hoechst nuclear staining. Images were captured using a confocal microscope with a 20× magnification objective. FSP1 immunopositive cells in each field were manually counted to support an assessment of the effect of various treatments relative to the respective controls.

Flow cytometry

HTM cells were seeded at 4×10^5 cells in $60cm^2$ plastic dishes and cultured as described above. Cells were infected with adenovirus expressing either GFP or RhoAV14/GFP at 50 MOI. When cultures exhibited adequate levels of infection (>80%, assessed based on GFP fluorescence) after 24-36 h following treatment with adenovirus, HTM cells were serum starved for 36 h. Cell suspensions were prepared after trypsinization (0.25% trypsin-EDTA), fixed with 1× fixation buffer (eBioscience, San Diego, CA), and permeabilized using Permeabilization Buffer (eBioscience). To minimize non-specific binding, cells were pre-blocked with blocking buffer containing 5% FBS in FACS buffer [FACS Buffer - 0.5% BSA (from Sigma) in 1× PBS]. Expression of α-SMA was assessed using a mouse monoclonal anti-α-SMA antibody conjugated to Cy3 and FSP-1 using rabbit anti-FSP-1 antibody with a secondary goat anti-rabbit Alexa Fluor 647. The specificity of staining was confirmed using mouse or rabbit-IgG2a isotype controls at the same concentration. The viability of cells was assessed using Fixable Viability Dye eFluor 450 (eBioscience). The cell suspensions were stained for 45 min with the primary and secondary antibodies and analyzed by flow cytometry (FACSCanto, Becton-Dickinson). For all the flow cytometry analyses, at least 10^4 cells were assessed per sample and only cells with forward and orthogonal light scatter characteristics similar to intact cells were included in the analysis. Experiments were performed in replicates of four using two different HTM cell strains. As multiple fluorochromes were used, compensation was performed to correct the spectral overlaps. The data were analyzed using FACSDiva Software (BD Biosciences, San Jose, CA).

Immunoblotting

Total protein cell lysates were prepared from serum-starved confluent cultures of HTM cells derived from the various experiments described. Protein assay reagent (Bio-Rad, Hercules, CA) was used to determine protein concentration of lysates. Samples containing equal amounts of protein were mixed with Laemmli buffer and separated by SDS-PAGE (8 and 15% acrylamide), followed by transfer of resolved proteins onto nitrocellulose membranes. Membranes were blocked for 2 h at room temperature in Tris-buffered saline containing 0.1% Tween 20 and 5% (wt/vol) nonfat dry milk and subsequently probed with primary antibodies (anti-αSMA, anti-FSP-1, anti-SMAD2/3, anti-pSMAD3, anti-FN, anti-Myc

(9E10), anti-GFP, anti-vimentin and anti-β–catenin) in conjunction with horseradish peroxidase-conjugated secondary antibodies. Detection of immunoreactivity was performed by enhanced chemiluminescence. Densitometry on immunoblot films was performed using NIH Image software. Data were normalized to the specified loading controls (anti-α– Tubulin, anti-β–Tubulin or anti-β–actin).

Sircol Assay

The amount of acid soluble collagen secreted into the medium was measured using the Sircol™ Assay (Accurate Chemicals, Westbury, NY) following the manufacturer's instructions. The Sircol assay is based on use of Sirius red, an anionic dye with sulphonic acid side chain groups that react with the side chain group of basic amino acids (imino acid hydroxyproline) present in collagen. In brief, HTM cells under test or control conditions were serum starved for at least 24 h prior to the experiment. Following appropriate treatments, the medium was removed and processed for the assay. Cold collagen isolation and concentration agent (200μl/mL of test sample) was added to cell culture media samples, mixed and incubated overnight at 4 °C. Samples were then centrifuged at 12,000g for 10 min at room temperature, supernatants drained, and 1.0 ml of Sircol Dye Reagent added to each pellet. Unbound dye was removed by ice-cold acid-salt wash. The collagen bound dye was then released using Alkali reagent and 200 μl of the solution was pipetted into a 96-well plate and absorbance was measured at 540 nm using a Spectramax M3 microplate reader (Molecular Devices, Sunnyvale, CA). Collagen standards were run simultaneously and used to determine the collagen content of different samples.

Statistical analyses

All data represent the average results of a minimum of three independent experiments. Quantitative data were analyzed by the Student's t-test, and a $p < 0.05$ was used to define statistically significant differences between test and control samples.

RESULTS

Effects of constitutively active RhoA, LPA, TGF-β2 and CTGF on HTM cell fibrogenic activity

To explore the potential influence of RhoA on the propensity of HTM cells to transdifferentiate into myofibroblast-like cells and to induce fibrogenic response, HTM cells were infected with adenovirus expressing either a constitutively active RhoA (RhoAV14 mutant) and GFP or GFP alone. After confirming the expression of GFP (at more than 80% efficiency based on GFP fluorescence), cells were serum starved for 36 h and used for either extraction of total RNA for q-PCR analysis, fixed for immunofluorescence analysis, flow cytometry or for preparation of cell lysates for immunoblot analysis. In these different analyses, we focused on changes in the expression profile or protein levels of three well-recognized biomarkers of myofibroblasts including Fibroblast Specific Protein-1 (FSP-1), αSMA and collagen-1A1. As we reported earlier, (Pattabiraman and Rao, 2010; Zhang et al., 2008) the RhoAV14 expressing cells revealed a robust increase in rhodamine-phalloidin stained actin stress fibers in conjunction with a stiffer or contractile cell morphology, relative to GFP expressing controls (data not shown). Fig. 1A shows significant increases (2 fold) in levels of FSP-1, αSMA and collagen-1A1 expression in the RhoAV14 expressing HTM cells as compared to GFP expressing control cells based on q-PCR analysis. These observations were based on the use of two independent HTM cell strains (primary cultures derived from two different human donors aged 58 and 73 years old) and triplicate analysis of each cell strain (n=6). The q-PCR–based observations were further validated by semi-quantitative RT-PCR analyses as shown in Fig. 1B. For each individual gene, an appropriate linear range RT-PCR cycles was used for semi-quantitative analyses. Consistent with the

results of q-PCR analysis (Fig. 1A), RT-PCR analysis also confirmed an increase in levels of expression of FSP-1, αSMA and collagen-1A1 in the RhoAV14 expressing HTM cells as shown in Fig. 1B (two independent specimens analyzed from both control and test groups).

HTM cell cultures expressing RhoAV14 showed a significantly increased number of cells staining positively for FSP-1 based on immunofluorescence analysis compared to GFP expressing control cells (Fig.1C and 1E; n=4 from two different donor cell lines). RhoAV14 expressing HTM cultures exhibit a similar robust increase in the number of cells immunostaining positively for both αSMA (Fig. 1C) and collagen-1A1 (Fig. 2A) compared to control cells expressing the GFP gene alone. These observations were validated independently by immunoblot analysis and flow cytometry. The levels of FSP-1 and αSMA proteins were significantly increased in HTM cells expressing the constitutively active form of RhoA based on quantitative immunoblot analysis (Fig. 1F and 1G; n=4). These observations were also found to be consistent with the results of flow cytometry analysis, which confirmed increased levels of FSP-1 (~19%) and αSMA (~30%) expression (Fig. 1H) in the RhoAV14 expressing cells relative to GFP controls with a significant number of cells co-expressing both FSP-1 and αSMA (~20%) under the conditions of Rho GTPase activation (Fig. 1H). Moreover, consistent to increased collagen-1A1 protein levels in RhoAV14 expressing HTM cells (Fig. 2A), the levels of secretory total collagen determined by the Sircol assay based on hydroxyproline specific dye-binding method revealed significantly elevated levels in the RhoAV14 expressing cells compared to the GFP expressing control HTM cells (Fig. 2C). Also in RhoAV14 expressing HTM cells, the expression status of HE4 (human epididymis protein-4), a protease inhibitor which has been identified recently as a biomarker of activated myofibroblasts and fibrosis (LeBleu et al., 2013) showed a robust increase (> 2 fold) as compared to respective GFP expressing control cells based on both q-PCR and RT-PCR analyses (Fig. 1A&B suppl.).

In addition to the above described direct effects of constitutively active RhoA on the expression pattern of myofibroblast and fibrogenic markers in HTM cells, we evaluated the effects of LPA (5 μM), TGF-β2 (10 ng/ml) and CTGF (40 ng/ml) on expression of FSP-1, αSMA, collagen-1A1 and secretory collagen. These physiological agents (LPA, TGF-β2 and CTGF) have been reported to activate Rho GTPase and influence the contractile properties of TM cells (Iyer et al., 2012b; Junglas et al., 2012; Mettu et al., 2004; Nakamura et al., 2002; Pattabiraman and Rao, 2010). Furthermore, the levels of these physiological agents or activity of enzymes producing some of these agents have been documented to be elevated in AH derived from glaucoma patients (Crean et al., 2011; Iyer et al., 2012a; Tripathi et al., 1994). Therefore, we examined the effects of LPA, TGF-β2 and CTGF on the levels of αSMA, FSP-1 and collagen-1A1 by immunofluorescence and immunoblot analysis. Consistent with the effects manifested upon expression of RhoAV14, treatment of serum starved HTM cells with these three physiological agents for 24 h resulted in significant increases in levels of FSP-1, αSMA and collagen-1A1 (Fig. 1D, E, F and G) and secretory total collagen (Fig. 2B, C) as compared to untreated controls. The number of FSP-1 expressing cells was significantly higher as determined by FSP-1 specific immunofluorescence of HTM cells treated with LPA, TGF-β2 or CTGF, as compared to untreated cells (Fig. 1E).

All the HTM cell strains derived from different donor eyes used in this study were evaluated for macrophage and microglial markers by immunofluorescence analysis using antibodies specific to F4/80 and Iba-1. No positive staining was detected for these markers (data not shown) in any of HTM cells used in this study.

SRF-MRTF-A interaction is critical for the RhoA-induced changes in expression of myofibroblast and fibrogenic markers in HTM cells

Rho GTPase has been demonstrated to enhance expression of αSMA and collagen-1A1 by activating the serum response factor (SRF) in different cell types (Cen et al., 2004; Mack et al., 2001; Pipes et al., 2006; Small, 2012; Wang et al., 2006). SRF-mediated transcriptional activation depends on the interaction of SRF with the co-activator myocardin-related transcription factor (MRTF-A and MRTF-B, also known as MAL and MKL1/2) in a G-actin dependent manner (Medjkane et al., 2009; Morita et al., 2007; Olson and Nordheim, 2010; Posern and Treisman, 2006). To assess the role of the SRF-MRTF interaction in HTM cell transition to myofibroblast phenotype and fibrogenic activity, we expressed recombinant EGFP-MRTF-A in HTM cells using plasmid based nucleofection and followed the changes in the expression profile of FSP-1, αSMA and collagen-1A1 by q-PCR, RT-PCR and immunofluorescence analyses. Both q-PCR and RT-PCR analyses revealed a significant increase in the expression of profibrotic genes FSP-1, collagen-1A1 and αSMA in cells expressing MRTF-A (Fig. 3A, B; n=6). Additionally, immunofluorescence analysis of the MRTF-A expressing HTM cells revealed a greater number of cells exhibiting positive staining for αSMA, FSP-1 and collagen-1A1 as compared to the control cells expressing EGFP-C1 alone (Fig. 3C).

To further assess the importance of SRF-MRTF interaction in regulating expression of myofibroblast and fibrogenic markers in TM cells, we took two different approaches to disrupt this interaction: chemical inhibition with CCG 1423 (10 μM), and suppression of SRF expression using a shRNA against SRF. Consistent to the previous observations shown in Fig. 1, the presence of LPA (5μM) or TGF-β2 (10ng/ml) alone for 24 h was able to increase the number of αSMA, FSP-1 and collagen-1A1 expressing cells (Fig. 3D) and significantly increased the levels of αSMA and FSP-1 in HTM cells (Fig. 3E and F; n=4). However, in the presence of CCG 1423, LPA and TGF-β2 failed to increase the number of αSMA, FSP-1 and collagen-1A1 expressing cells and the levels of αSMA and FSP-1 in HTM cells as determined by immunofluorescence and immunoblot analyses respectively (Fig. 3D, E and F; n=4). Treatment with CCG 1423 (10 μM) alone showed no significant effects on the basal levels of αSMA and FSP-1. Additionally, HTM cells treated with CCG 1423 for 24 h in the presence of LPA (5 μM) or TGF-β2 (10 ng/ml) did not exhibit changes in levels of secretory total collagen as assessed by the Sircol assay compared to the controls (Fig. 3G). On the other hand, consistent with the previous observation (Fig. 1), both LPA and TGF-β2 significantly increased the levels of secretory total collagen in HTM cells (Fig. 3G; n=4).

We also targeted SRF expression using shRNA against SRF and assessing its effect on the expression profile of myofibroblast and fibrogenic markers in HTM cells. Adenovirus-mediated expression of shRNA against SRF (shSRF) significantly knocked down SRF protein (by >80%) as we have reported earlier (data not shown) compared to the shGFP-transduced control (Pattabiraman and Rao, 2010). Treatment of HTM cells transduced with shGFP control with LPA (5μM) or TGF-β2 (10ng/ml) alone for 24 h yielded an increase in the number of αSMA, collagen-1A1 and FSP-1 expressing cells based on immunofluorescence analysis (Fig. 4A). However, in cells expressing shRNA against SRF, LPA or TGF-β2 failed to elicit an increase in expression of αSMA, collagen-1A1 and FSP-1 (Fig. 4A) as compared to the shGFP controls. LPA (5μM) or TGF-β2 (10ng/ml)-induced increases in secretory total collagen was also suppressed upon shRNA-mediated downregulation of SRF expression (Fig. 4B; n=4) indicating the importance of SRF in regulation of expression of collagen in HTM cells.

RhoA and MRTF regulate expression of transcriptional suppressors involved in regulation of cell plasticity and transdifferentiation in HTM cells

To explore whether RhoA and MRTF exert transcriptional influence on TM cell plasticity or fate transition in the context of myofibroblast generation, we evaluated the expression profile of transcriptional repressors involved in regulating the transition of epithelial or endothelial cells to myofibroblast-like cells (EMT or EndMT) including Slug, Snail and Twist-1 in HTM cells (Kalluri and Weinberg, 2009; Zeisberg and Neilson, 2009). HTM cells (derived from both 58 and 73 year-old donors) infected with RhoAV14 expressing adenovirus (for a period of 36 h) or transfected with plasmids expressing MRTF-A, exhibited significant increases in expression of Slug and Twist-1 based on q-PCR and RT-PCR analyses as compared to the GFP expressing controls (Fig. 5A, B; n=6). Under similar conditions however, expression of Snail was found to be significantly downregulated upon the expression of recombinant RhoAV14 or MRTF-A as compared to GFP controls (Fig. 5A, B; n=6).

We then examined the effects of expressing recombinant Slug on the expression profile of myofibroblast biomarkers and regulators of cell-cell interactions in HTM cells. To address this objective, a full length version of Slug (Slug-Myc tagged) was expressed in HTM cells together with an EGFP-C1 control. Expression of the Myc-Slug and EGFP-C1 was confirmed by immunofluorescence staining for Myc-tagged Slug and GFP fluorescence (not shown) and by Myc and GFP immunoblot analysis (Fig. 5C). HTM cells expressing recombinant Slug showed a significant increase in the levels of αSMA and fibronectin and an increase in intermediate filament vimentin based on immunoblot analysis (Fig. 5C, D; n=3). On the other hand, the levels of β-catenin were decreased significantly in Slug expressing HTM cells as compared to the control cells expressing GFP. Additionally, cell shape of HTM cells expressing recombinant Slug appeared longer with more pronounced cell-cell separation as compared to the controls (Fig.2 Suppl).

Effects of RhoA and TGF-β2 on the expression profile of miRNA29 in HTM cells

MicroRNAs, which are small non-coding RNA molecules, have been recognized as critical regulators of gene expression. To determine the influence of RhoA, MRTF-A and TGF-β2 on the expression profile of miRNA29 and miRNA21 which are known to regulate expression of certain ECM molecules involved in fibrosis (Chau et al., 2012; Cushing et al., 2011; Kumarswamy et al., 2012; Pandit et al., 2011; van Rooij et al., 2008), HTM cells expressing recombinant RhoAV14, MRTF-A or treated with TGF-β2 (10ng/ml) for 24 h, were subjected to q-PCR analysis to quantify the levels of miRNA29a, miRNA29b and miRNA21. These analyses revealed that while the expression of miRNA29b and miRNA21 was unaltered, miRNA29a levels were significantly increased in HTM cells expressing RhoAV14, MRTF-A or cells treated with TGF-β2 as compared to the respective controls (Fig. 6). These observations were based on the use of two independent donor HTM cell strains with each one with triplicate analyses. U26 small nucleolar RNA (RNU26) was used to normalize the amount of DNA used in q-PCR analysis.

Role of RhoA and SMAD3 in TGF-β2-induced αSMA expression in HTM cells

To determine the involvement of SMADs and RhoA in mediating the effects of TGF-β2 on αSMA expression in TM cells, we employed the SMAD2/3 inhibitor SIS3 (10 μM for 6 h) and RhoA inhibitor (C3 toxin; 1μg/ml for 6 h) alone or along with the stimulation of TGF-β2 (10 ng/ml for 6 h). The levels of SMAD2/3, phospho-SMAD3 and αSMA were probed by immunoblotting. A significant increase occurred in SMAD3 phosphorylation in TGF-β2 stimulated HTM cells, with no significant change in the levels of total SMAD2 and SMAD3 (Fig. 7A & B). In contrast, the TGF-β2 induced SMAD3 phosphorylation was decreased significantly in cells pretreated with SIS3 (Fig. 7A & B). Pretreatment of cells with SIS3 led

to a partial but significant dampening of the TGF-β2 mediated increase in αSMA expression relative to the TGF-β2 treated controls (Fig. 7A & B). On the other hand, pretreatment of HTM cells with RhoA inhibitor-C3 toxin significantly and completely decreased the induction of αSMA by TGF-β2, but was without effect on TGF-β2-induced SMAD3 phosphorylation (Fig. 7A & B). These observations were based on four independent analyses.

Rho kinase inhibitor-Y27632 and anti-fibrotic agent-Pirfenidone inhibit TGF-β2-induced fibrogenic activity in HTM cells

Based on above described observations on the role of RhoA and TGF-β2 signaling in TM cell fibrogenic activity, we tested the effects of Rho kinase inhibition on the expression profile of fibrogenic and myofibroblast markers induced by TGF-β2 in HTM cells. Additionally, we compared the effects of Rho kinase inhibition with the effects of a known anti-fibrotic agent Pirfenidone on the expression of fibrogenic and myofibroblast markers. Serum starved HTM cells treated with TGF-β2 (10 ng/ml) along with the presence of Rho kinase inhibitor-Y27632 (10 μM) or Pirfenidone (2.5 mM) for 24 h showed a marked decrease in the expression of αSMA, FSP-1 and collagen-1A1 compared to cells treated with TGF-β2 alone, based on immunofluorescence analysis (Fig. 8A). Treatment of HTM cells with either Y-27632 or Pirfenidone alone could suppress the expression of αSMA, FSP-1 and collagen-1A1 as compared to untreated controls based on immunofluorescence analysis as shown in Fig. 8A. In addition to immunofluorescence analysis, immunoblot analysis was performed to confirm these observations. Consistent with the results obtained from immunofluorescence analysis, treatment of HTM cells with Rho kinase inhibitor (Y-27632) or Pirfenidone led to significant decreases in the levels of TGF-β2-induced expression of αSMA and FSP-1 (Fig. 8B, 8C). Additionally, the TGF-β2-induced increase in levels of secretory total collagen was significantly decreased by Y-27632 and Pirfenidone compared to cells treated with TGF-β2 alone (Fig. 8D). These results were based on 4 independent analyses.

DISCUSSION

To explore the hypothesis that dysregulated contractile mechanotransduction associated with activated Rho GTPase signaling induces aberrant fibrogenic activity in TM cells, we systematically evaluated the effects of constitutively active Rho GTPase and physiological activators of Rho GTPase signaling on the propensity of HTM cells to transdifferentiate into myofibroblast-like cells expressing fibrogenic and fibroblast-like markers. These cell-based experiments revealed augmented expression of various biomarkers of myofibroblast and fibrogenic activity in HTM cells under the conditions of activation of Rho GTPase signaling. Importantly, these changes were found to be mediated by the SRF-MRTF transcriptional axis and Slug and Twist, which are transcriptional suppressors of cell adhesive proteins and control cell plasticity. Moreover, Rho GTPase/Rho kinase signaling appears to play a significant role in TGF-β2 induced fibrogenic activity in HTM cells, and inhibition of Rho kinase activity suppressed the expression of both fibrogenic and myofibroblast specific markers induced by TGF-β2 in HTM cells.

Rho GTPase activation in TM cells has been found to stimulate robust increases in cellular contraction in association with increased myosin II phosphorylation, actin stress fibers, and induce expression of genes encoding αSMA, TGF-β2, CTGF, IL-1 and various ECM proteins in a Rho kinase dependent manner (Iyer et al., 2012b; Pattabiraman and Rao, 2010; Zhang et al., 2008). Moreover, ECM proteins have been shown to activate Rho GTPase signaling and contraction in TM cells through a feed forward loop mechanism (Zhang et al., 2008). Along with these changes, significantly, expression of constitutively active RhoA in the AH outflow pathway and perfusion of enucleated eyes with LPA, a potent activator of

Rho GTPase signaling, both have been found to increase resistance to AH outflow (Mettu et al., 2004; Zhang et al., 2008). Since Rho GTPase induced changes in cell shape, actomyosin interaction and contractile-mechanotransduction are known to influence cell plasticity, fate transition and fibrogenic activity (Arnsdorf et al., 2009; Berndt et al., 2008; Ingber, 2003; McBeath et al., 2004; Small et al., 2010; Zhou et al., 2013), we attempted to further delineate the role of Rho GTPase signaling in modulating TM cell characteristics in the context of AH outflow. To this end, we tested the effects of Rho GTPase activation on the phenotypic acquisition of TM cells to myofibroblast-like cells by following the expression pattern of myofibroblast markers. Developmentally, TM cells are derived from neural crest-derived periocular mesenchymal cells and possess endothelial-like characteristics (Alvarado et al., 2004; Liu and Johnson, 2010). Constitutively active RhoA (RhoAV14), LPA, TGF-β2 and CTGF, which have been demonstrated to activate Rho GTPase and induce actin stress fiber formation in TM cells (Junglas et al., 2012; Mettu et al., 2004; Nakamura et al., 2002; Pattabiraman and Rao, 2010), were found to increase both the expression and protein levels of myofibroblast markers FSP-1, αSMA and collagen-1A1 in HTM cells (Kalluri and Neilson, 2003; Zeisberg and Neilson, 2009). Additionally, the levels of total secretory collagen were also significantly increased under the above described conditions. RhoAV14 also stimulated increased expression of HE4, a newly characterized biomarker of myofibroblasts and fibrosis, in HTM cells (LeBleu et al., 2013). Collectively these initial observations encouraged us to hypothesize that Rho activation status might influence TM cell plasticity and fibrogenic activity.

Consistent with observations described above, our previous studies using HTM cells documented the ability of RhoAV14, LPA and TGF-β2 to elicit increases in not only αSMA and fibronectin but SRF as well (Pattabiraman and Rao, 2010). SRF is a well-characterized transcription factor that interacts with the serum response element of various immediate-early genes to regulate gene expression, development and various other cellular processes (Medjkane et al., 2009; Posern and Treisman, 2006). Moreover, the transcriptional activity of SRF has been demonstrated to be regulated by Rho GTPase signaling and actin cytoskeletal organization (Posern and Treisman, 2006). Significantly, expression of both αSMA and collagen-1A1 is known to be regulated by SRF (Pattabiraman and Rao, 2010; Pipes et al., 2006; Small, 2012; Wang et al., 2006; Zhao et al., 2007). SRF transcriptional activity is closely linked to that of its co-activator myocardin-related transcription factor (MRTF), in a G-actin dependent manner (Olson and Nordheim, 2010; Posern and Treisman, 2006; Small et al., 2010). Therefore, we evaluated the role of both MRTF-A and SRF on TGF-β2 and LPA induced expression of fibrogenic and myofibroblast markers in HTM cells. Expression of recombinant MRTF-A per se induced expression of FSP-1, αSMA and collagen-1A1 revealing the direct influence of MRTF-A on cell plasticity and transdifferentiation of TM cells into FSP-1 and αSMA expressing myofibroblast like cells. Significantly, inhibition of the interaction of MRTF-A with SRF via use of CCG1423 or suppression of SRF expression by shRNA, led to a marked decrease in expression of LPA- and TGF-β2-induced expression of FSP-1, αSMA and collagen-1A1 in HTM cells. Collectively, these observations demonstrated a definitive role for the Rho GTPase regulated actin-SRF-MRTF axis transcriptional activity in mediating the TM cell fibrogenic activity and acquisition of myofibroblast-like phenotype.

In addition to SRF and MRTF, the Snail family of zinc finger transcription factors including Snail and Slug, have been shown to regulate mesoderm formation and cell fate transition (Kalluri and Weinberg, 2009; Kokudo et al., 2008; Medici et al., 2011; Morita et al., 2007; Shields et al., 2012). Both Snail and Slug and related proteins from this family act as transcriptional suppressors to control the expression of cell-cell junctional proteins such as E-cadherin and thereby influence cell fate transition (Alves et al., 2009; Kalluri and Weinberg, 2009; Peinado et al., 2007). Moreover, Rho GTPase, TGF-β and SRF/MRTF are

known to influence the expression of Snail, Slug and Twist-1 in different cell types during EMT and EndMT processes (Mihira et al., 2012; Morita et al., 2007; Ridley and Hall, 2004; Shields et al., 2012). In experiments designed to determine the potential role of RhoA and MRTF-A in regulating the expression profile of transcriptional suppressors in TM cells, we found that RhoAV14 and MRTF-A each supported significant increases in expression of both Slug and Twist-1 in HTM cells. Moreover, expression of recombinant Slug in HTM cells led to a significant increase in the levels of αSMA, fibronectin and vimentin. In contrast, the levels of adherens junction-interacting β-catenin were decreased in HTM cells under similar conditions, consistent with the observed phenotypic changes in HTM cell morphology and cell-cell separation in Slug expressing cells. These observations suggest the participation of different transcriptional suppressors in regulation of cell-cell adhesive interactions during TM cell fate transition, and a critical role for Rho GTPase and SRF/ MRTF in regulation of Slug and Twist-1 expression in TM cells. To additionally explore the possible involvement of miRNAs in RhoAV14 and TGF-β2 stimulated TM cells, we examined the changes in levels of well characterized miRNAs including miRNA29a, miRNA29b and miRNA21 involved in regulation of fibrogenic activity in different cell types (Chau et al., 2012; Cushing et al., 2011; van Rooij et al., 2008). Intriguingly, while decreased levels of miRNA29 are commonly noted to be associated with increased levels of ECM during fibrosis, (Cushing et al., 2011; van Rooij et al., 2008) HTM cells expressing RhoAV14, MRTF-A or treated with TGF-β2 exhibited elevated levels of miRNA29a in association with increased levels of collagen-1A1 and total collagen with no changes in miRNA29b and miRNA21. Further studies are necessary to understand the increased levels of miRNA29a under activation of Rho GTPase and TGF-β2 in TM cells.

In these studies, we also determined the relative importance of Rho GTPase signaling and the canonical signaling pathway mediated by SMADs in TGF-β2 induced fibrogenic activity in TM cells. These mechanistic studies however, revealed a much stronger influence of RhoA in the TGF-β2 induced αSMA expression in HTM cells relative to SMAD2/3. This observation is consistent with previous reports on the significance of Rho GTPase signaling in TGF-β induced αSMA expression, transdifferentiation and fibrogenic activity in different cell types (Bhowmick et al., 2001; Cho and Yoo, 2007; Masszi et al., 2003; Nakamura et al., 2002; Small, 2012). Further evidence for the participation of Rho GTPase and Rho kinase signaling in TM cell fibrogenic activity was deduced from the significant decrease in the TGF-β2-induced expression of αSMA, FSP-1 and collagen-1A1 in the presence of Rho kinase inhibitor (Y-27632) in HTM cells. Additionally, a well-characterized anti-fibrotic agent Pirfenidone (Carter, 2011; Iyer et al., 1999) also suppressed the fibrogenic response induced by TGF-β2 in HTM cells.

Collectively, based on these different and consistent observations, it is reasonable to conclude that activation of Rho GTPase signaling in the TM cells and other cell types of the AH outflow pathway can lead to changes in cell plasticity, myofibroblast generation/ activation and fibrogenic activity via heightened contractile mechanosensitive signaling and transcriptional activity. These changes are expected to ultimately influence the biomechanical properties and stiffness of TM cells and AH outflow facility due to dysregulated accumulation of ECM proteins. In contrast, the Rho kinase inhibitors appear to prevent or suppress the fibrogenic activity perhaps by decreased cell tension and thereby enhance AH outflow facility and possess ocular hypotensive activity. Studies are underway to explore and validate the potential role(s) of fibrogenic mechanisms in the RhoAV14 induced ocular hypertension rat model and human glaucoma subjects.

Supplementary Material

Refer to Web version on PubMed Central for supplementary material.

Acknowledgments

Abbreviations used in the figure legends

FSP-1	Fibroblast specific protein-1
Col1A1	Collagen -1A1
αSMA	alpha-smooth muscle actin
GFP	green fluorescent protein
q-PCR	quantitative polymerase cycle reaction
RT-PCR	reverse transcriptase polymerase cycle reaction
HTM	human trabecular meshwork
GAPDH	glycerol 3 phosphate dehydrogenase
CTGF	connective tissue growth factor
LPA	lysophosphatidic acid
TGF-β2	transforming growth factor-beta 2
SRF	serum response factor
MRTF	myocardin-related transcription factor
miRNA	microRNA
SD	standard deviation

REFRENCES

Alvarado JA, Betanzos A, Franse-Carman L, Chen J, Gonzalez-Mariscal L. Endothelia of Schlemm's canal and trabecular meshwork: distinct molecular, functional, and anatomic features. Am J Physiol Cell Physiol. 2004; 286(3):C621–634. [PubMed: 14613887]

Alves CC, Carneiro F, Hoefler H, Becker KF. Role of the epithelial-mesenchymal transition regulator Slug in primary human cancers. Front Biosci. 2009; 14:3035–3050.

Arnsdorf EJ, Tummala P, Kwon RY, Jacobs CR. Mechanically induced osteogenic differentiation--the role of RhoA, ROCKII and cytoskeletal dynamics. J Cell Sci. 2009; 122(Pt 4):546–553. [PubMed: 19174467]

Berndt JD, Clay MR, Langenberg T, Halloran MC. Rho-kinase and myosin II affect dynamic neural crest cell behaviors during epithelial to mesenchymal transition in vivo. Dev Biol. 2008; 324(2): 236–244. [PubMed: 18926812]

Bhowmick NA, Ghiassi M, Bakin A, Aakre M, Lundquist CA, Engel ME, Arteaga CL, Moses HL. Transforming growth factor-beta1 mediates epithelial to mesenchymal transdifferentiation through a RhoA-dependent mechanism. Mol Biol Cell. 2001; 12(1):27–36. [PubMed: 11160820]

Carter NJ. Pirfenidone: in idiopathic pulmonary fibrosis. Drugs. 2011; 71(13):1721–1732. [PubMed: 21902295]

Cen B, Selvaraj A, Prywes R. Myocardin/MKL family of SRF coactivators: key regulators of immediate early and muscle specific gene expression. J Cell Biochem. 2004; 93(1):74–82. [PubMed: 15352164]

Chau BN, Xin C, Hartner J, Ren S, Castano AP, Linn G, Li J, Tran PT, Kaimal V, Huang X, Chang AN, Li S, Kalra A, Grafals M, Portilla D, MacKenna DA, Orkin SH, Duffield JS. MicroRNA-21 promotes fibrosis of the kidney by silencing metabolic pathways. Sci Transl Med. 2012; 4(121): 121ra118.

Cho HJ, Yoo J. Rho activation is required for transforming growth factor-beta-induced epithelial-mesenchymal transition in lens epithelial cells. Cell Biol Int. 2007; 31(10):1225–1230. [PubMed: 17537651]

Crean JK, Browne JG, Ho SL, Kane R, Oliver N, Clark AF, O'Brien CJ. Connective Tissue Growth Factor Is Increased in Pseudoexfoliation Glaucoma. Invest Ophthalmol Vis Sci. 2011; 52(6):3660–3666. [PubMed: 21330667]

Cushing L, Kuang PP, Qian J, Shao F, Wu J, Little F, Thannickal VJ, Cardoso WV, Lu J. miR-29 is a major regulator of genes associated with pulmonary fibrosis. Am J Respir Cell Mol Biol. 2011; 45(2):287–294. [PubMed: 20971881]

de Kater AW, Shahsafaei A, Epstein DL. Localization of smooth muscle and nonmuscle actin isoforms in the human aqueous outflow pathway. Invest Ophthalmol Vis Sci. 1992; 33(2):424–429. [PubMed: 1740375]

Flugel C, Tamm E, Lutjen-Drecoll E. Different cell populations in bovine trabecular meshwork: an ultrastructural and immunocytochemical study. Exp Eye Res. 1991; 52(6):681–690. [PubMed: 1855543]

Fuchshofer R, Tamm ER. The role of TGF-beta in the pathogenesis of primary open-angle glaucoma. Cell Tissue Res. 2012; 347(1):279–290. [PubMed: 22101332]

Gabelt BT, Kaufman PL. Changes in aqueous humor dynamics with age and glaucoma. Prog Retin Eye Res. 2005; 24(5):612–637. [PubMed: 15919228]

Honjo M, Tanihara H, Inatani M, Kido N, Sawamura T, Yue BY, Narumiya S, Honda Y. Effects of rho-associated protein kinase inhibitor Y-27632 on intraocular pressure and outflow facility. Invest Ophthalmol Vis Sci. 2001; 42(1):137–144. [PubMed: 11133858]

Ingber DE. Tensegrity II. How structural networks influence cellular information processing networks. J Cell Sci. 2003; 116(Pt 8):1397–1408. [PubMed: 12640025]

Iyer P, Lalane R 3rd, Morris C, Challa P, Vann R, Rao PV. Autotaxin-lysophosphatidic acid axis is a novel molecular target for lowering intraocular pressure. PLoS One. 2012a; 7(8):e42627. [PubMed: 22916143]

Iyer P, Maddala R, Pattabiraman PP, Rao PV. Connective tissue growth factor-mediated upregulation of neuromedin U expression in trabecular meshwork cells and its role in homeostasis of aqueous humor outflow. Invest Ophthalmol Vis Sci. 2012b; 53(8):4952–4962. [PubMed: 22761259]

Iyer SN, Gurujeyalakshmi G, Giri SN. Effects of pirfenidone on transforming growth factor-beta gene expression at the transcriptional level in bleomycin hamster model of lung fibrosis. J Pharmacol Exp Ther. 1999; 291(1):367–373. [PubMed: 10490926]

Junglas B, Kuespert S, Seleem AA, Struller T, Ullmann S, Bosl M, Bosserhoff A, Kostler J, Wagner R, Tamm ER, Fuchshofer R. Connective tissue growth factor causes glaucoma by modifying the actin cytoskeleton of the trabecular meshwork. Am J Pathol. 2012; 180(6):2386–2403. [PubMed: 22542845]

Kalluri R, Neilson EG. Epithelial-mesenchymal transition and its implications for fibrosis. J Clin Invest. 2003; 112(12):1776–1784. [PubMed: 14679171]

Kalluri R, Weinberg RA. The basics of epithelial-mesenchymal transition. J Clin Invest. 2009; 119(6): 1420–1428. [PubMed: 19487818]

Keller KE, Aga M, Bradley JM, Kelley MJ, Acott TS. Extracellular matrix turnover and outflow resistance. Exp Eye Res. 2009; 88(4):676–682. [PubMed: 19087875]

Kokudo T, Suzuki Y, Yoshimatsu Y, Yamazaki T, Watabe T, Miyazono K. Snail is required for TGFbeta-induced endothelial-mesenchymal transition of embryonic stem cell-derived endothelial cells. J Cell Sci. 2008; 121(Pt 20):3317–3324. [PubMed: 18796538]

Kumarswamy R, Volkmann I, Jazbutyte V, Dangwal S, Park DH, Thum T. Transforming growth factor-beta-induced endothelial-to-mesenchymal transition is partly mediated by microRNA-21. Arterioscler Thromb Vasc Biol. 2012; 32(2):361–369. [PubMed: 22095988]

Kwon YH, Fingert JH, Kuehn MH, Alward WL. Primary open-angle glaucoma. N Engl J Med. 2009; 360(11):1113–1124. [PubMed: 19279343]

LeBleu VS, Teng Y, O'Connell JT, Charytan D, Muller GA, Muller CA, Sugimoto H, Kalluri R. Identification of human epididymis protein-4 as a fibroblast-derived mediator of fibrosis. Nat Med. 2013; 19(2):227–231. [PubMed: 23353556]

Liu P, Johnson RL. Lmx1b is required for murine trabecular meshwork formation and for maintenance of corneal transparency. Dev Dyn. 2010; 239(8):2161–2171. [PubMed: 20568247]

Lutjen-Drecoll E, Shimizu T, Rohrbach M, Rohen JW. Quantitative analysis of 'plaque material' in the inner- and outer wall of Schlemm's canal in normal- and glaucomatous eyes. Exp Eye Res. 1986; 42(5):443–455. [PubMed: 3720863]

Mack CP, Somlyo AV, Hautmann M, Somlyo AP, Owens GK. Smooth muscle differentiation marker gene expression is regulated by RhoA-mediated actin polymerization. J Biol Chem. 2001; 276(1):341–347. [PubMed: 11035001]

Masszi A, Di Ciano C, Sirokmany G, Arthur WT, Rotstein OD, Wang J, McCulloch CA, Rosivall L, Mucsi I, Kapus A. Central role for Rho in TGF-beta1-induced alpha-smooth muscle actin expression during epithelial-mesenchymal transition. Am J Physiol Renal Physiol. 2003; 284(5):F911–924. [PubMed: 12505862]

McBeath R, Pirone DM, Nelson CM, Bhadriraju K, Chen CS. Cell shape, cytoskeletal tension, and RhoA regulate stem cell lineage commitment. Dev Cell. 2004; 6(4):483–495. [PubMed: 15068789]

McKee CT, Wood JA, Shah NM, Fischer ME, Reilly CM, Murphy CJ, Russell P. The effect of biophysical attributes of the ocular trabecular meshwork associated with glaucoma on the cell response to therapeutic agents. Biomaterials. 2011; 32(9):2417–2423. [PubMed: 21220171]

Medici D, Potenta S, Kalluri R. Transforming growth factor-beta2 promotes Snail-mediated endothelial-mesenchymal transition through convergence of Smad-dependent and Smad-independent signalling. Biochem J. 2011; 437(3):515–520. [PubMed: 21585337]

Medjkane S, Perez-Sanchez C, Gaggioli C, Sahai E, Treisman R. Myocardin-related transcription factors and SRF are required for cytoskeletal dynamics and experimental metastasis. Nat Cell Biol. 2009; 11(3):257–268. [PubMed: 19198601]

Mettu PS, Deng PF, Misra UK, Gawdi G, Epstein DL, Rao PV. Role of lysophospholipid growth factors in the modulation of aqueous humor outflow facility. Invest Ophthalmol Vis Sci. 2004; 45(7):2263–2271. [PubMed: 15223804]

Mihira H, Suzuki HI, Akatsu Y, Yoshimatsu Y, Igarashi T, Miyazono K, Watabe T. TGF-beta-induced mesenchymal transition of MS-1 endothelial cells requires Smad-dependent cooperative activation of Rho signals and MRTF-A. J Biochem. 2012; 151(2):145–156. [PubMed: 21984612]

Morita T, Mayanagi T, Sobue K. Dual roles of myocardin-related transcription factors in epithelial mesenchymal transition via slug induction and actin remodeling. J Cell Biol. 2007; 179(5):1027–1042. [PubMed: 18056415]

Nakamura Y, Hirano S, Suzuki K, Seki K, Sagara T, Nishida T. Signaling mechanism of TGF-beta1-induced collagen contraction mediated by bovine trabecular meshwork cells. Invest Ophthalmol Vis Sci. 2002; 43(11):3465–3472. [PubMed: 12407157]

Olson EN, Nordheim A. Linking actin dynamics and gene transcription to drive cellular motile functions. Nat Rev Mol Cell Biol. 2010; 11(5):353–365. [PubMed: 20414257]

Pandit KV, Milosevic J, Kaminski N. MicroRNAs in idiopathic pulmonary fibrosis. Transl Res. 2011; 157(4):191–199. [PubMed: 21420029]

Pattabiraman PP, Rao PV. Mechanistic basis of Rho GTPase-induced extracellular matrix synthesis in trabecular meshwork cells. Am J Physiol Cell Physiol. 2010; 298(3):C749–763. [PubMed: 19940066]

Peinado H, Olmeda D, Cano A. Snail, Zeb and bHLH factors in tumour progression: an alliance against the epithelial phenotype? Nat Rev Cancer. 2007; 7(6):415–428. [PubMed: 17508028]

Pipes GC, Creemers EE, Olson EN. The myocardin family of transcriptional coactivators: versatile regulators of cell growth, migration, and myogenesis. Genes Dev. 2006; 20(12):1545–1556. [PubMed: 16778073]

Posern G, Treisman R. Actin' together: serum response factor, its cofactors and the link to signal transduction. Trends Cell Biol. 2006; 16(11):588–596. [PubMed: 17035020]

Rao PV, Deng PF, Kumar J, Epstein DL. Modulation of aqueous humor outflow facility by the rho kinase-specific inhibitor Y-27632. Invest Ophthalmol Vis Sci. 2001; 42(5):1029–1037. [PubMed: 11274082]

Rao PV, Deng PF, Sasaki Y, Epstein DL. Regulation of myosin light chain phosphorylation in the trabecular meshwork: role in aqueous humour outflow facility. Exp Eye Res. 2005; 80(2):197–206. [PubMed: 15670798]

Ridley AJ, Hall A. Snails, Swiss, and serum: the solution for Rac 'n' Rho. Cell. 2004; 116(2 Suppl):S23–25. 22, S25. [PubMed: 15055577]

Rosenthal R, Choritz L, Schlott S, Bechrakis NE, Jaroszewski J, Wiederholt M, Thieme H. Effects of ML-7 and Y-27632 on carbachol- and endothelin-1-induced contraction of bovine trabecular meshwork. Exp Eye Res. 2005; 80(6):837–845. [PubMed: 15939040]

Russell P, Johnson M. Elastic modulus determination of normal and glaucomatous human trabecular meshwork. Invest Ophthalmol Vis Sci. 2012; 53(1):117.

Shields MA, Krantz SB, Bentrem DJ, Dangi-Garimella S, Munshi HG. Interplay between beta1-integrin and Rho signaling regulates differential scattering and motility of pancreatic cancer cells by snail and Slug proteins. J Biol Chem. 2012; 287(9):6218–6229. [PubMed: 22232555]

Small EM. The actin-MRTF-SRF gene regulatory axis and myofibroblast differentiation. J Cardiovasc Transl Res. 2012; 5(6):794–804. [PubMed: 22898751]

Small EM, Thatcher JE, Sutherland LB, Kinoshita H, Gerard RD, Richardson JA, Dimaio JM, Sadek H, Kuwahara K, Olson EN. Myocardin-related transcription factor-a controls myofibroblast activation and fibrosis in response to myocardial infarction. Circ Res. 2010; 107(2):294–304. [PubMed: 20558820]

Tamm ER, Fuchshofer R. What increases outflow resistance in primary open-angle glaucoma? Surv Ophthalmol. 2007; 52(Suppl 2):S101–104. [PubMed: 17998032]

Tamm ER, Siegner A, Baur A, Lutjen-Drecoll E. Transforming growth factor-beta 1 induces alpha-smooth muscle-actin expression in cultured human and monkey trabecular meshwork. Exp Eye Res. 1996; 62(4):389–397. [PubMed: 8795457]

Tektas OY, Lutjen-Drecoll E. Structural changes of the trabecular meshwork in different kinds of glaucoma. Exp Eye Res. 2009; 88(4):769–775. [PubMed: 19114037]

Tripathi RC, Li J, Chan WF, Tripathi BJ. Aqueous humor in glaucomatous eyes contains an increased level of TGF-beta 2. Exp Eye Res. 1994; 59(6):723–727. [PubMed: 7698265]

van Rooij E, Sutherland LB, Thatcher JE, DiMaio JM, Naseem RH, Marshall WS, Hill JA, Olson EN. Dysregulation of microRNAs after myocardial infarction reveals a role of miR-29 in cardiac fibrosis. Proc Natl Acad Sci U S A. 2008; 105(35):13027–13032. [PubMed: 18723672]

Wang J, Zohar R, McCulloch CA. Multiple roles of alpha-smooth muscle actin in mechanotransduction. Exp Cell Res. 2006; 312(3):205–214. [PubMed: 16325810]

Weinreb RN, Khaw PT. Primary open-angle glaucoma. Lancet. 2004; 363(9422):1711–1720. [PubMed: 15158634]

Wiederholt M, Thieme H, Stumpff F. The regulation of trabecular meshwork and ciliary muscle contractility. Prog Retin Eye Res. 2000; 19(3):271–295. [PubMed: 10749378]

Yue BY. The extracellular matrix and its modulation in the trabecular meshwork. Surv Ophthalmol. 1996; 40(5):379–390. [PubMed: 8779084]

Zeisberg EM, Tarnavski O, Zeisberg M, Dorfman AL, McMullen JR, Gustafsson E, Chandraker A, Yuan X, Pu WT, Roberts AB, Neilson EG, Sayegh MH, Izumo S, Kalluri R. Endothelial-to-mesenchymal transition contributes to cardiac fibrosis. Nat Med. 2007; 13(8):952–961. [PubMed: 17660828]

Zeisberg M, Kalluri R. Cellular mechanisms of tissue fibrosis. 1. Common and organ-specific mechanisms associated with tissue fibrosis. Am J Physiol Cell Physiol. 2013; 304(3):C216–225. [PubMed: 23255577]

Zeisberg M, Neilson EG. Biomarkers for epithelial-mesenchymal transitions. J Clin Invest. 2009; 119(6):1429–1437. [PubMed: 19487819]

Zhang M, Maddala R, Rao PV. Novel molecular insights into RhoA GTPase-induced resistance to aqueous humor outflow through the trabecular meshwork. Am J Physiol Cell Physiol. 2008; 295(5):C1057–1070. [PubMed: 18799648]

Zhao XH, Laschinger C, Arora P, Szaszi K, Kapus A, McCulloch CA. Force activates smooth muscle alpha-actin promoter activity through the Rho signaling pathway. J Cell Sci. 2007; 120(Pt 10): 1801–1809. [PubMed: 17456553]

Zhou Y, Huang X, Hecker L, Kurundkar D, Kurundkar A, Liu H, Jin TH, Desai L, Bernard K, Thannickal VJ. Inhibition of mechanosensitive signaling in myofibroblasts ameliorates experimental pulmonary fibrosis. J Clin Invest. 2013; 123(3):1096–1108. [PubMed: 23434591]
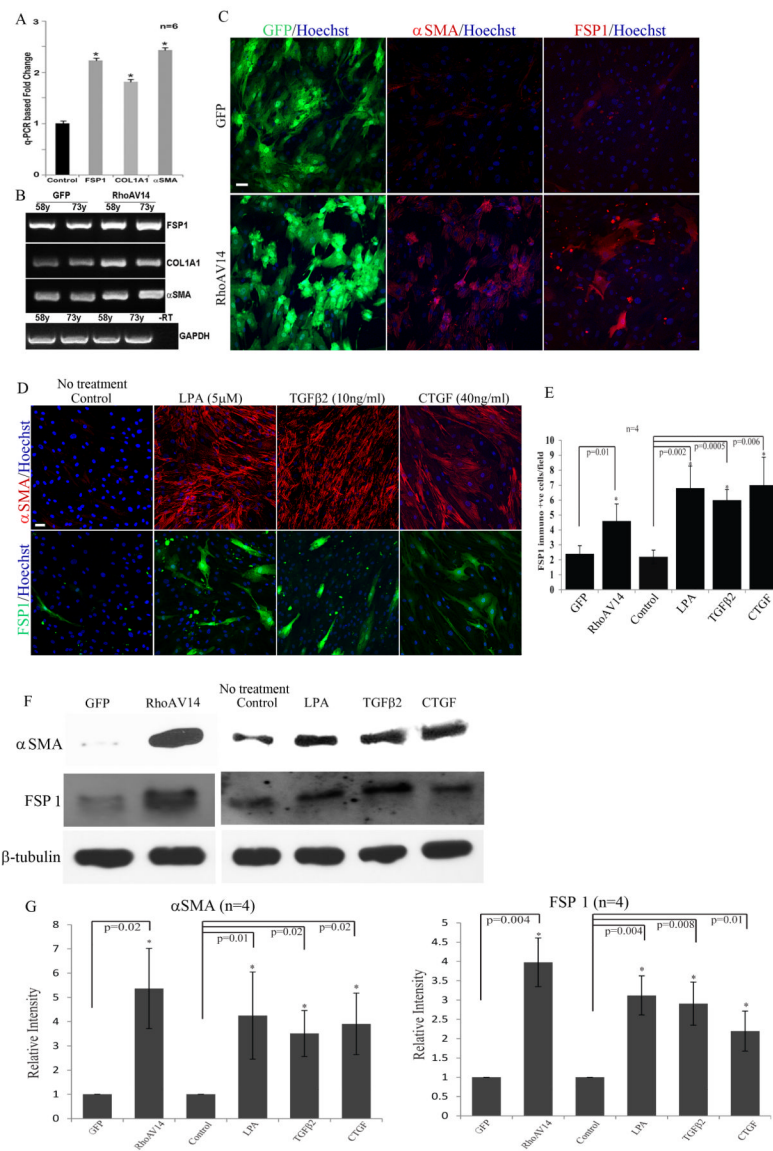
Figure 1.

Constitutively active RhoA (RhoAV14)-induced expression of fibrogenic and myofibroblast markers in HTM cells.
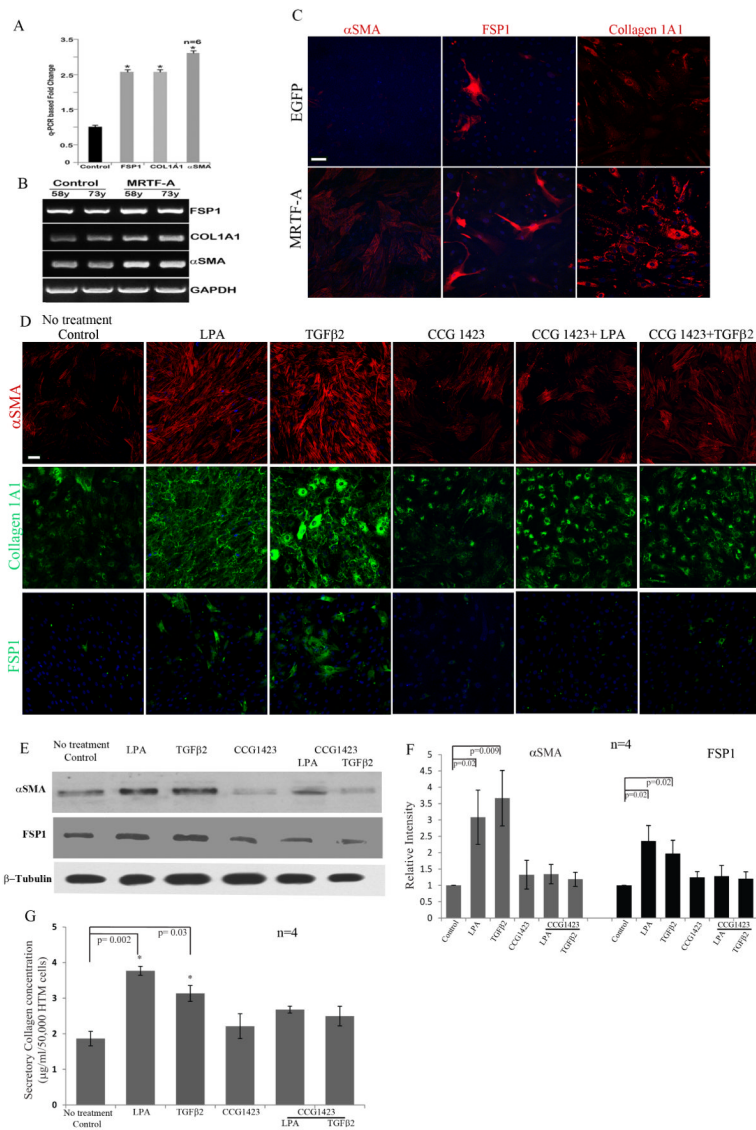
A. Analysis of total RNA from serum starved HTM cells (derived from 58 and 73 years old donor eyes) expressing recombinant RhoAV14/GFP by q-PCR revealed a significant increase in expression of FSP-1, collagen-1A1 (Col1A1) and αSMA as compared to GFP expressing control cells. Values represent mean ± SD of two independent experiments performed in triplicate. * P<0.05. **B**. Semi-quantitative RT-PCR analysis of the same samples described in panel A shows the relative increase in expression of FSP-1, collagen-1A1 (Col1A1) and αSMA in the RhoAV14 expressing HTM cells compared to GFP expressing controls. Expression of GAPDH was used as a normalizing control. –RT represents a sample of RT-PCR reaction performed in the absence of reverse transcriptase. **C.** Representative images depicting increased immunofluorescence staining for αSMA and FSP1 in serum starved HTM cells infected with adenovirus expressing recombinant RhoAV14/GFP, relative to GFP expressing controls. Scale bar: 50μm. **D.** Treatment of

serum starved HTM cells with LPA (5μM), TGF-β2 (10 ng/ml) and CTGF (40 ng/ml) for 24 h induces expression of αSMA and FSP1 as evaluated by immunofluorescence analysis. Scale bar: 50μm. **E**. Quantitative changes in number of FSP-1 immunopositive cells under the above described treatments based on manual counting. Values represent Mean± SD (n=4). * P<0.05. **F** and **G** show significantly increased levels of αSMA and FSP-1, respectively in the RhoAV14 expressing and LPA, TGF-β2 and CTGF treated HTM cells based on immunoblot analysis with subsequent densitometric analysis. β-Tubulin was immunoblotted as a loading control (n=4, Mean± SD) * P<0.05. **H** shows significantly increased expression of αSMA and FSP-1 in RhoAV14 expressing HTM cells relative to GFP expressing controls based on Flow cytometry analysis. Results are expressed as relative percent of cells immunostained positively for the respective proteins, based on 4 independent analyses. Lower panel depicts the significantly higher relative percent values of RhoAV14 cells exhibiting co-distribution of αSMA and FSP-1 relative to GFP expressing controls.
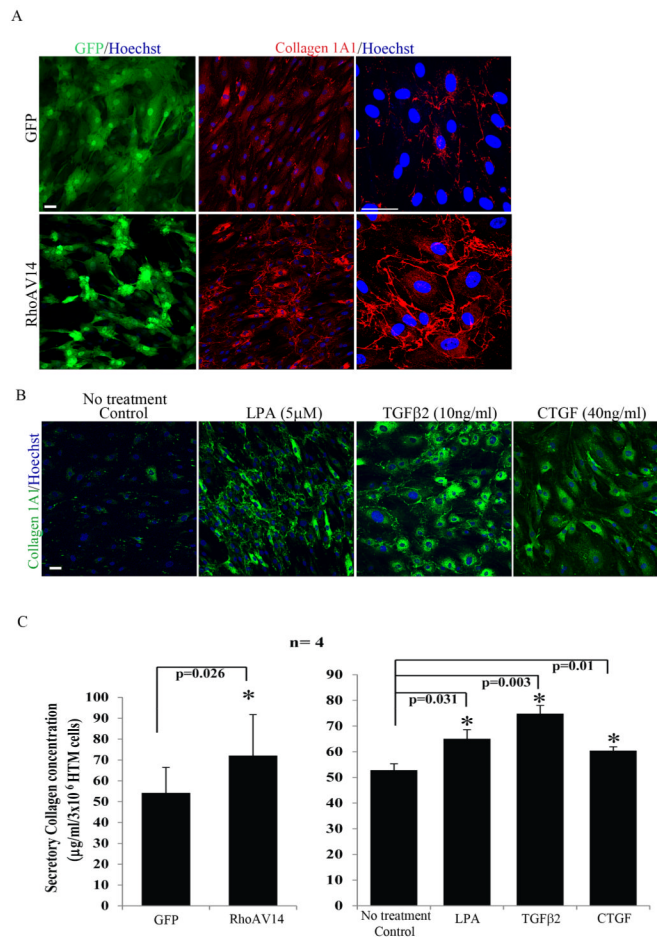
Figure 2.
Increased production of Collagen by RhoAV14 expressing, and TGF-β2, LPA and CTGF treated HTM cells.

A. Serum starved RhoAV14/GFP expressing cells exhibit a relatively higher number of cells immunopositive for collagen as compared to cells expressing the GFP alone. Panels on right show higher magnification images revealing increased accumulation of collagen-1A1 in the RhoAV14 expressing cells. Scale bar: 50μm. **B**. Serum starved HTM cells treated with LPA (5μM), TGF-β2 (10ng/ml) or CTGF (40ng/ml) for 24 h exhibit relatively higher numbers of cells staining positive for Col1A1 based on immunofluorescence staining. Scale bar: 50μm. C. Panel C shows significantly higher levels of secretory total collagen in the RhoAV14 expressing, and LPA, TGF-β2 and CTGF treated HTM cells as compared to their respective controls determined by the Sircol assay. Values represent Mean± SD of 4 individual analyses. * P<0.05.

Figure 3.
Effects of MRTF-A, a transcriptional co-activator of serum response factor (SRF) and inhibitor of MRTF-A (CCG1423) on HTM cell fibrogenic activity.
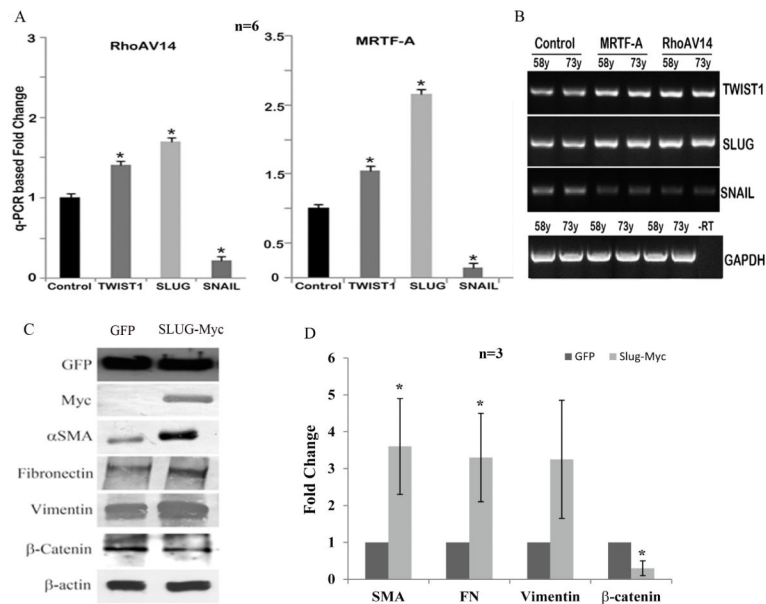
A. Total RNA derived from serum starved HTM cells (derived from two different human donors; age 58 and 73 year-old) expressing recombinant MRTF-A was subjected to q-PCR to detect changes in gene expression levels for FSP-1, collagen-1A1 and αSMA. Expression of all three genes was significantly elevated in MRTF-A expressing cells compared to GFP expressing control cells. GAPDH expression was used to normalize the cDNA content of test samples. Data represent values from two independent experiments performed in triplicates (n=6, Mean± SD) * P<0.05. **B**. Analysis of the same cDNAs described above (A) by semi-quantitative RT-PCR analysis revealed that the expression of FSP-1, collagen-1A1 (Col1A1) and αSMA was relatively higher in the MRTF-A expressing HTM cells as compared to the control cells. **C**. Serum starved HTM cells expressing recombinant MRTF-A exhibited a relatively higher number of cells staining positive for αSMA, FSP-1 and collagen-1A1 based on immunofluorescence analysis, and compared to control cells transfected with GFP. Scale bar: 50μm. **D**. Serum starved HTM cells treated with CCG 1423

(10μM) alone or in combination with LPA (5μM) or TGF-β2 (10 ng/ml) for 24 h showed a markedly reduced staining for αSMA, Col 1A1 and FSP-1 as compared to LPA and TGF-β2 treated HTM cells based on immunofluorescence analysis. Representative images from 4 independent analyses are shown. Scale bar: 50μm. **E** and **F**. Under similar conditions as mentioned above, changes in the levels of αSMA and FSP-1 were assessed by immunoblot analysis, and consistent with the changes noted above, there was a significant increase in the levels αSMA and FSP-1 in response to treatment with LPA and TGF-β2. However, the levels of both αSMA and FSP-1 were reduced significantly in the presence of CCG1423, in LPA and TGF-β2 treated cells. Histograms depict the relative changes in the levels of αSMA and FSP-1 based on densitometric analysis. Values represent Mean± SD of 4 independent experiments. * P<0.05. β-Tubulin was immunoblotted as a loading control. **G**. CCG1423 causes significant decreases in the levels of secreted collagen induced by LPA and TGF-β2 treatment of HTM cells, as compared to the respective controls, based on the Sircol assay. Values represent Mean± SD of 4 independent experiments. * P<0.05.
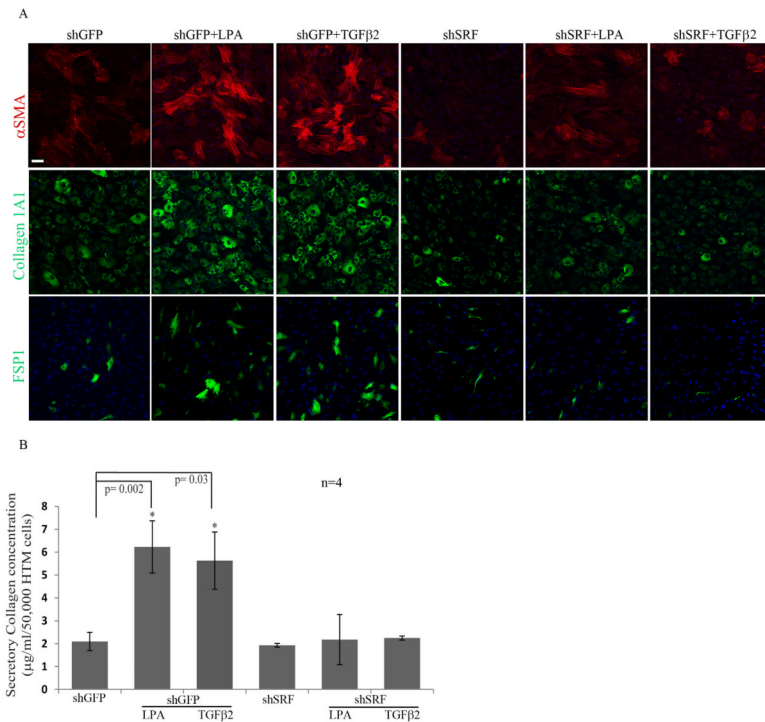
Figure 4.
Silencing of SRF expression decreases the expression of αSMA, collagen-1A1 and FSP-1, and levels of secretory total collagen in HTM cells.

**A**. HTM cells expressing the shRNA against SRF were found to exhibit a dramatic reduction in the LPA-(5μM) and TGF-β2 (10 ng/ml)-induced expression of αSMA, Col 1A1 and FSP-1 as compared to respective LPA and TGF-β2 treated cells. shRNA targeted SRF expression per se in HTM cells also showed a reduction in the number of cells exhibiting positive staining for αSMA, FSP-1 and collagen-1A1 as compared to GFP expressing control cells. Representative images from 4 individual analyses were shown. Scale bar: 50μm. **B**. Under similar conditions as described in panel A, levels of secretory total collagen were reduced significantly in HTM cells with decreased expression of SRF, both in the presence and absence of LPA and TGF-β2, and as compared to the respective controls. Values represent Mean± SD of 4 independent samples. * P<0.05.

Figure. 5.
Regulation of expression of transcriptional suppressors-Slug, Snail and Twist-1 in HTM cells and effects of Slug on HTM cell plasticity and fibrogenic activity.
A. Total RNA derived from serum starved HTM cells (derived from two different human donors: 58 and 73 year-old) expressing either RhoAV14 or recombinant MRTF-A were subjected to q-PCR analysis to detect relative changes in gene expression for Snail, Slug and Twist-1. Cells expressing either RhoAV14 or MRTF-A exhibit a significant increase in the expression of Slug and Twist-1 as compared to the respective controls. Interestingly, under similar conditions, the levels of Snail expression were reduced significantly. Data represent two independent experiments in triplicates (n=6, Mean± SD) * P<0.05. **B**. The q-PCR based observations described in panel A were further validated using a semi-quantitative RT-PCR analysis using the same specimens. –RT represents a sample of RT-PCR reaction performed in the absence of reverse transcriptase. **C** and **D.** To determine the effects of Slug on TM cell plasticity and fibrogenic activity, HTM cells expressing the recombinant myc-tagged Slug were examined for changes in the levels of αSMA, fibronectin, vimentin and β-catenin. EGFP expressing cells were used as controls. Serum starved HTM cells expressing recombinant Slug showed a significant increase in the levels of αSMA and fibronectin and an increase in vimentin as compared to EGFP expressing controls based on immunoblot analysis. Myc was probed to confirm the expression of recombinant Slug in the HTM cells and GFP was probed for transfection efficiency. In contrast to fibronectin, vimentin and αSMA, the levels of β-catenin were reduced significantly in the Slug expressing HTM cells. Values are based on n=3 and represent mean ±SD.
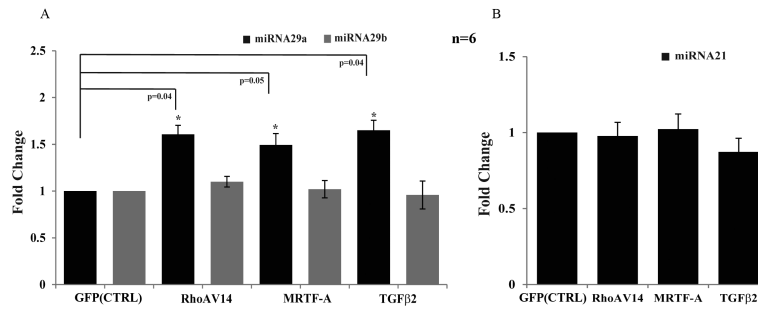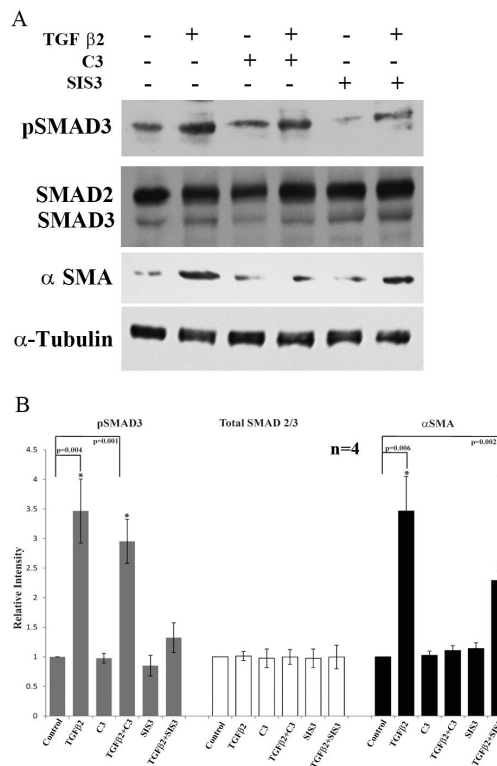
Figure 6.
Influence of RhoA, MRTF-A and TGF-β2 on the expression profile of miRNA29a, b and miRNA21 in HTM cells.

RNA derived from the serum starved HTM cells expressing either the recombinant RhoAV14, MRTF-A or treated with TGF-β2 (10ng/ml) for 24 h was subjected to q-PCR to detect the relative changes in expression of miRNA29a, miRNA29b (A) and miRNA21 (B). While the levels of miRNA29b and miRNA21 were unaltered, there was a significant increase in miRNA29a expression in the cells expressing RhoAV14 and MRTF-A, or treated with TGF-β2 as compared to respective controls. RNA samples were normalized to the expression of U26 small nucleolar RNA (RNU26). Data represent values from two independent experiments in triplicates (n=6, Mean± SD) * P<0.05.

Figure 7.
Relative involvement of Rho GTPase and SMAD3 in TGF-β2 induced expression of αSMA in HTM cells.

A. Serum starved HTM cells were treated with TGF-β2 (10ng/ml) alone or in the presence of RhoA inhibitor-C3 (1µg/ml for 6 h) or inhibitor of SMAD3 phosphorylation-SIS3 (10µM for 6 h) and examined for changes in the levels of phospho-SMAD3, total SMAD3/SMAD2 and αSMA by immunoblot analysis using the respective antibodies. For loading controls, α-tubulin was immunoblotted. As shown in panels **A** and **B,** TGF-β2 induced SMAD3 phosphorylation as expected in HTM cells, and this response was reduced significantly in the presence of SIS3. On the other hand, in the presence of C3 (RhoA inhibitor), the levels of phospho-SMAD3 were still significantly elevated in the TGF-β2 treated cells, but the levels of αSMA which were increased significantly in response to TGF-β2, decreased to normal levels in the presence of C3. Although the levels of αSMA were reduced in cells treated with SIS3, they were still significantly higher as compared to untreated controls. The levels of total SMAD2/3 were not affected by any of the treatments described above. Histograms in panel B indicate the densitometry-based values from an average (Mean± SD) of 4 independent experiments. * P<0.05.
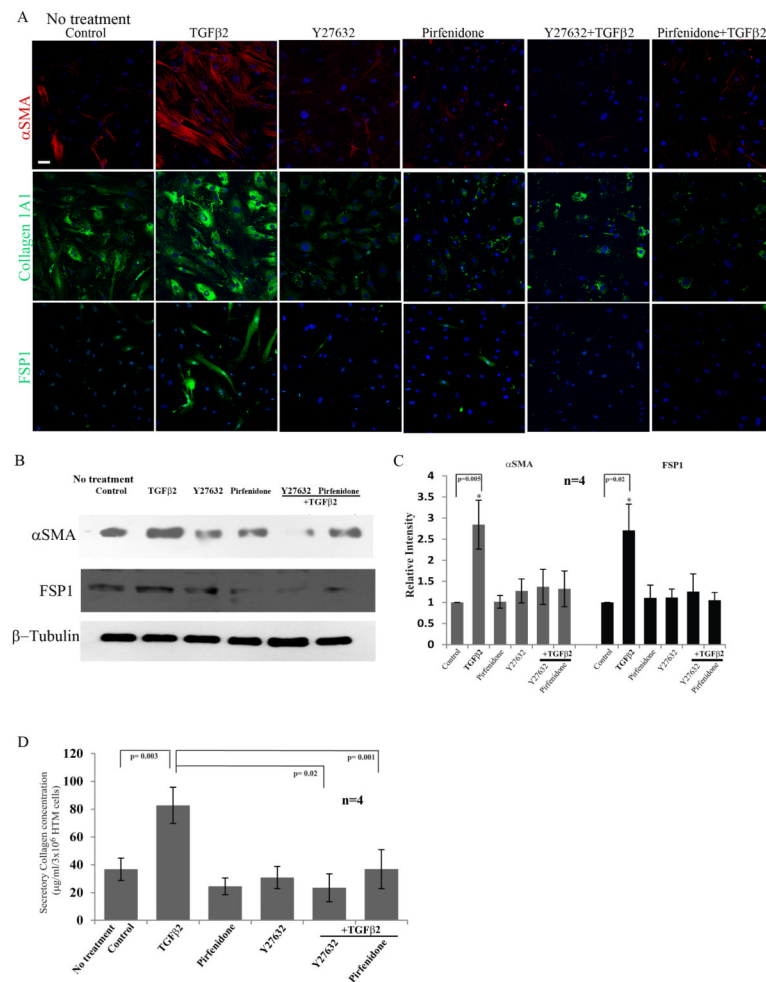
Figure 8.

Rho kinase inhibitor-Y27632 and anti-fibrotic agent-Pirfenidone suppress the fibrogenic activity induced by TGF-β2 in HTM cells.

A. Serum starved HTM cells treated with TGF-β2 (10 ng/ml for 24 h) exhibited increased expression of αSMA, collagen-1A1 and FSP-1 based on immunofluorescence analysis. This response was suppressed when the cells were treated along with Y-27632 (10 μM) or Pirfenidone (2.5 mM) and TGF-β2. Representative images of 4 independent analyses were shown. Scale bar: 50μm. **B** and **C**. Under similar conditions as described above, the levels of αSMA and FSP-1 which were increased significantly in the presence of TGF-β2 showed no change from the untreated cells in the presence of Y-27632 or Pirfenidone, as determined by immunoblot analysis. Histograms represent the densitometry-based values from an average (Mean± SD) of 4 independent experiments. * P<0.05. β-Tubulin was immunoblotted as loading control. **D**. Consistent with above described effects of Y-27632 and Pirfenidone on TGF-β2 induced changes in αSMA and FSP-1, the levels of secretory total collagen determined by the Sircol assay were found to be unaltered in the presence of Y-27632 and Pirfenidone in the TGF-β2 treated cells. On the other hand, TGF-β2 by itself significantly increased the levels of secretory collagen in HTM cells as compared to untreated control cells. Both Pirfenidone and Y27632 also caused some reduction (not significant) in the basal levels of secretory collagen compared to the control. (n=4, Mean± SD) * P<0.05.

TABLE 1

Oligonucleotide primers used in the RT-PCR and q-PCR amplifications

Gene Name	Forward primer	Reverse Primer	Product size (bps)
FSP1	GAGAAGGCCCTGGATGTGAT	CCTCGTTGTCCCTGTTGCTG	192
SMA	CTGTTCCAGCCATCCTTCAT	CCGTGATCTCCTTCTGCATT	175
Col1A1	GAGAGCATGACCGATGGATT	CCTTCTTGAGGTTGCCAGTC	185
SNAIL	GGCTCCTTCGTCCTTCTCCTCTAC	CTGGAGATCCTTGGCCTCAGAGAG	124
SLUG	CATGCCTGTCATACCACAAC	GGTGTCAGATGGAGGAGGG	169
TWIST	CGGGAGTCCGCAGTCTTA	TGAATCTTGCTCAGCTTGTC	150
HE4	GTTCGGCTTCACCCTAGTC	CACCTTCCCACAGCCATT	295
GAPDH	TGCACCACCAACTGCTTAGC	GGCATGGACTGTGGTCATGAG	90